Received: 21 December 2023 | Revised: 10 May 2024 | Accepted: 2 June 2024

DOI: 10.1111/geb.13881

Global Ecology and Biogeography A Journal of Macroecology WILEY

RESEARCH ARTICLE

The rise and fall of shark functional diversity over the last 66 million years

Jack A. Cooper[1] | **Catalina Pimiento**[1,2]

[1]Department of Biosciences, Swansea University, Swansea, UK

[2]Department of Paleontology, University of Zurich, Zurich, Switzerland

Correspondence
Jack A. Cooper, Department of Biosciences, Swansea University, Wallace Building, Singleton Park, Sketty, Swansea, SA2 8PP, Wales, UK.
Email: jackacooper33@gmail.com

Funding information
University of Florida [International travel grant]; Fisheries Society of the British Isles [PhD studentship]; Swiss National Science Foundation [PRIMA], Grant/Award Number: 185798

Handling Editor: Kathleen Lyons

Abstract

Aim: Modern sharks are a diverse and highly threatened group playing important roles in ecosystems. They have an abundant fossil record spanning at least 250 million years (Myr), consisting primarily of isolated teeth. Throughout their evolutionary history, sharks have faced multiple environmental changes and extinction events. Here, we aim to use dental characters to quantify how shark functional diversity has changed during the last 66 Myr.

Location: Global.

Time period: Cenozoic era (66–0 million years ago; Ma).

Major taxa studied: Sharks (Selachii).

Methods: We complied a dataset of over 9000 shark teeth belonging to 537 taxa from museum collections and scientific literature and measured six dental characters strongly linked with functional traits. We then quantified different functional diversity metrics across Cenozoic time bins, compared them against null expectations and identified the most important taxa contributing to maintaining functional diversity.

Results: Sharks displayed relatively high functional diversity during the Cenozoic, with 66%–87% of the functional space being occupied for ~60 Myr (Palaeocene to Miocene). High levels of functional redundancy during this time resulted in larger-than-expected functional richness; but a large decline (−45%) in redundancy in the Oligocene (~30 Ma) left shark functional diversity highly vulnerable to further loss. Shark functional diversity declined from the late Miocene (~10 Ma) onwards, losing 44% of functional richness by the Recent. Extinct sharks disproportionally contributed to the Cenozoic functional diversity and spanned a wider range of functional space than extant sharks, with the loss of mid-sized suction feeders and large-bodied predators driving functional declines.

Main conclusions: After maintaining high levels of functional diversity for most of the Cenozoic, sharks lost nearly half of their functional diversity in the last ~10 Myr. Current anthropogenic pressures are therefore likely eroding an already diminished shark functional diversity, leaving future communities ecologically deprived compared with their thriving geological past.

KEYWORDS
Cenozoic, dental characters, extinction, functional diversity, sharks, traits

1 | INTRODUCTION

Sharks (Elasmobranchii, Selachii) are a diverse and ecologically disparate group of marine vertebrates (Compagno, 1990). With over 500 living species across nearly all marine habitats (Weigmann, 2016), they play a range of critical functions in marine systems such as apex predators controlling prey populations (Myers et al., 2007), mesopredators acting as food sources for larger predators (Navia et al., 2017) and nutrient transporters connecting distant populations and habitats (Williams et al., 2018). Notably, modern sharks are evolutionary distinct compared to other marine vertebrates (Stein et al., 2018) and have a 250-million-year-old fossil record consisting mostly of well-preserved teeth, which are highly abundant in marine sediments worldwide (Cappetta, 2012; Kent, 1994).

Throughout their long evolutionary history, sharks have experienced numerous environmental changes and survived several extinction events (Belben et al., 2017; Guinot et al., 2012; Guinot & Condamine, 2023; Kriwet & Benton, 2004; Sibert & Rubin, 2021). While previous studies have examined shark morphological disparity through time (Bazzi et al., 2021; Belben et al., 2017), how their functional diversity has changed remains largely unexplored. Exploring this question is possible by examining fossil shark teeth, which have been demonstrated to be good proxies of traits such as body size, prey preference and feeding mechanism (Cooper et al., 2023). Because these traits can reflect how sharks obtain and move resources across systems, they can be used as a basis to quantify the diversity of their ecological functions (herein, functional diversity; Mouillot et al., 2013).

Functional diversity can be assessed using different approaches. One approach involves quantifying the ecological functions in a community (i.e. number of unique trait combinations, or functional entities; herein, FEs) and the number of species filling them. This approach allows assessing the level of functional resilience in a community by measuring functional redundancy (i.e. number of species per entity; herein, FRed) and over-redundancy (i.e. % of species filling entities above the mean level of redundancy, which measures the over-representation of some functions; herein, FOred; Mouillot et al., 2013, 2014). Furthermore, functional diversity can be quantified based on the distribution of species in a multidimensional space defined by their traits (Mouillot et al., 2013; Villéger et al., 2008). Such an approach allows to quantify the range of ecological functions based on the volume of trait space occupied by a community (i.e. functional richness; herein, FRic; Mouillot et al., 2013). Similarly, the distribution of species in trait space allows identifying species possessing dissimilar or extreme traits. In this context, 'functional originality' is measured as the distance of species to their closest neighbour (herein, FOri) and 'functional specialization' is measured based on the distance of species to the centroid of the space (herein, FSpe; Mouillot et al., 2013), which in turn enables identifying species whose loss would result in disproportional declines of functional diversity (e.g. Pimiento et al., 2020). By assessing functional diversity using these different approaches, it is possible to quantify changes over time, identify the species contributing the most to maintaining ecological functions and quantify the potential ecological consequences of extinctions (Pimiento et al., 2017, 2020, 2023; Villéger et al., 2011).

Here, we use shark teeth to evaluate how shark functional diversity has changed throughout the Cenozoic, from 66 million years ago (Ma) to the present. We focus on this era as many shark taxa in the Cenozoic fossil record have living representatives (Paillard et al., 2020; Pimiento & Benton, 2020) and therefore, the tooth-trait links in extant sharks can be applied (Cooper et al., 2023). We first compiled a global image dataset of over 9000 shark teeth belonging to 537 taxa from which we took measurements of dental characters known to be proxies to ecological traits. We then characterized the structure of the shark functional space and calculated several functional diversity metrics across different time bins (i.e. geological epochs and stages) across the Cenozoic. We included a time bin representing the present-day (i.e. Recent), for which we only used extant species with a fossil record (i.e. 21.3% of extant species [Ebert et al., 2021]; see below) to allow a suitable comparison with the inherently incomplete fossil record. Finally, we quantified individual contributions to functional diversity to identify the taxa whose extinctions had the largest impacts and to determine whether extinct or extant taxa had larger contributions. Our results provide insights into the range of shark ecological functions through a significant portion of their long evolutionary history and provide a deep-time perspective to their present-day functional diversity.

2 | MATERIALS AND METHODS

2.1 | Data

2.1.1 | Specimen collection

We searched for shark tooth specimens spanning the Cenozoic era (66–0 Ma; Gradstein et al., 2012) and the present-time (i.e. the Recent). We did this from: (1) nine museum collections in which all specimens found were photographed with a scale bar to allow subsequent measurements; (2) images in online museum repositories and (3) tooth images from the literature (see supplementary methods). Literature was searched using Shark-References (https://shark-refer ences.com; last accessed May 2023; Pollerspöck & Straube, 2014), from which we could extract images from 208 scientific publications (Data S1). All images used in this data collection can be found in the Zenodo Repository (https://doi.org/10.5281/zenodo.10076354).

From each tooth, we recorded: (1) taxonomic information from museum labels or the scientific publications, which was corrected when necessary based on the taxonomy from Shark-References (Pollerspöck & Straube, 2014); (2) tooth position to account for heterodonty using museum labels or the publications where the specimen came from, and comparisons to associated dentitions from the literature and (3) geological information (i.e. longitude, latitude, formation, locality and age) from museum labels, the literature and the Palaeobiology Database (PBDB; https://paleobiodb.org/; last accessed May 2023). Age (epoch and stage) was assigned following Gradstein et al. (2012). Finally, we assessed whether a taxon was extinct or extant based on Shark-References (Pollerspöck & Straube, 2014) and the PBDB.

In total, we gathered images of 8595 Cenozoic fossil shark teeth belonging to 537 taxa, 454 identified to the species-level (75.6% of all Cenozoic fossil species; Pollerspöck & Straube, 2014) and 83 to the genus-level. We additionally collected images of 965 teeth of living sharks (i.e. from the Recent), 115 identified to species (21.5% of all known extant species; Ebert et al., 2021), and one to genus (Data S1). We then degraded our Recent sample to ensure that it was comparable to the fossil record (see below). Our data covered all continents; however, data distribution had a notable bias towards Europe and North America (Figure S1) given that eight of the nine museums visited were located in these continents; and the sampling of the fossil record is known to be highly skewed towards wealthy regions (Raja et al., 2022).

2.1.2 | Dental measurements

We examined the following six dental characters from each specimen collected: crown height, crown width, cutting edge, lateral cusplets, cross-section outline and longitudinal outline (Table S1). We chose these six characters as they were previously found to be proxies for three main ecological traits in extant sharks: body size, prey preference and feeding mechanism (Cooper et al., 2023). Specifically, tooth size (i.e. crown height and crown width) is a strong proxy for body size; tooth size and cutting edge are strong proxies for prey preference and all of these characters in addition to lateral cusplets and tooth shape (i.e. longitudinal outline and cross-section outline) are strong proxies for feeding mechanism (Table S2; Cooper et al., 2023). Crown height and crown width were measured directly from the specimens examined in museum collections using digital callipers (in mm), and from the images (which had a scale bar) using ImageJ (Abràmoff et al., 2004) for specimens collected from online museum repositories and the literature. The rest of the characters were categorical and assigned to each specimen based on a visual inspection. Dental characters were treated as either ordinal or nominal variables in our analyses (see supplementary methods).

2.1.3 | Time-binning

Based on the geological information collected from each specimen, we assigned each taxon a Cenozoic epoch (Palaeocene, 66–56 Ma; Eocene, 56–33.9 Ma; Oligocene, 33.9–23.03 Ma; Miocene, 23.03–5.333 Ma; Pliocene, 5.333–2.58 Ma and Pleistocene, 2.58–0.01 Ma; Gradstein et al., 2012). We excluded the Holocene (0.01–0 Ma) from our analyses because we only collected two fossil specimens from this epoch (a *Carcharodon carcharias* and an *Isurus* sp.). All present-day specimens were assigned to the Recent (0 Ma). To ensure that this sample is comparable with the rest of the Cenozoic, we followed Villéger et al. (2011) and only included extant taxa with a fossil record. We assessed whether an extant taxon had a fossil record based on Pimiento and Benton (2020) and Paillard et al. (2020), which resulted in the exclusion of 53 species.

We used a range-through approach to fill the gaps in non-consecutive epochs from each taxon's age range (e.g. if a taxon was recorded in the Oligocene and Pliocene, we assumed it was also present in the Miocene). Following this data treatment of the fossil record, we extended the range of all extant taxa to the Recent, even if they were not recorded from the present-day sample, except for genus-level taxa for which all their species were already present in the Recent, which were recorded as extinct. This resulted in the addition of 51 taxa to the Recent, 16 species and 35 genera, for a total of 114 taxa in the degraded Recent sample.

We additionally assigned each taxon to a Cenozoic stage and repeated the steps described above. This additional binning was done to (1) assess whether the uneven duration of geological epochs affected our results and (2) capture more detailed changes in functional diversity over time. However, our main analyses were done to the epoch level to facilitate interpretability due to the high number of geological stages (i.e. 22; Gradstein et al., 2012).

2.1.4 | Final dataset

The degradation of the Recent (i.e. including only extant taxa with a fossil record) resulted in a final dataset of 9178 shark teeth. The total number of taxa remained the same: 454 were identified to the species-level and 83 to the genus-level. Our dataset included 100% of the Cenozoic orders and families, 92% of the genera and 75.6% of the fossil species deemed to be valid by Shark-References (Pollerspöck & Straube, 2014). Our degraded Recent sample included 85% of extant taxa known to have a fossil record (Paillard et al., 2020) and 21.3% of all living shark species (Ebert et al., 2021; Weigmann, 2016). We consider this acceptable for our comparison with the fossil record as we cannot assume that the Cenozoic sample represents the true shark diversity of the geological past due to the inherently incomplete fossil record (Benton et al., 2011; Foote & Sepkoski, 1999; Marshall, 2019). Nevertheless, given our relatively low representation of current diversity in the Recent sample, we performed additional analyses to assess how the inclusion of additional living taxa affects our results (see below).

2.2 | Analyses

2.2.1 | Trait analyses

All analyses were conducted in the R environment (R Core Team 2017). Association between tooth position and each dental character was tested to assess the influence of monognathic (within jaws) and dignathic (between jaws) heterodonty. To do so, we used polychoric correlations (Table S3) in the *DescTools* package (Signorell et al., 2019). All dental characters (Table S1) were found to have weak associations with tooth position (*rho* <0.35; Table S3), suggesting that heterodonty does not influence our results.

2.2.2 | Iterative functional taxonomic units

Shark tooth morphology can display intraspecific variation due to differences in life stage, sex and jaw position (Cappetta, 2012; Cullen & Marshall, 2019; Kent, 1994). To account for intraspecific variation in tooth morphology, and hence in functional traits (Albert et al., 2012; Cianciaruso et al., 2009; de Bello et al., 2011), we quantified all different dental character combinations per taxon. We refer to these as Functional Taxonomic Units (FTUs; Pimiento et al., 2017). A total of 1442 FTUs were computed across 537 taxa. However, in order to retain the taxonomic identity of each FTU, we performed the functional diversity analyses described below using one randomly selected FTU per taxon and repeating this process across 1000 iterations.

2.2.3 | Functional diversity analyses

We used two approaches to quantify functional diversity, one based on unique trait combinations, or functional entities (FEs; Mouillot et al., 2013, 2014) and one based on the distribution of taxa in a multidimensional trait space (Mouillot et al., 2013; Villéger et al., 2008). All functional diversity metrics under both approaches were computed using the *mFD* package (Magneville et al., 2022) and were computed per time bin and across each FTU iteration (see above).

For the first approach, we first quantified the number of functional entities (i.e. FE richness) per time bin using the 'sp.to.fe' function. We identified a total of 122 FEs, corresponding to 5.65% of a possible 2160. Then, based on the number of FEs per iteration (see above), we used the 'alpha.fd.fe' function to calculate functional redundancy (i.e. FRed; the average number of taxa per entity) and over-redundancy (i.e. FOred; % of taxa that fill FEs above the mean level of redundancy) per time bin.

For the second approach, we created a multidimensional functional space based on the dental characters assigned to each taxon (Mouillot et al., 2013). To do so, we first computed a trait distance matrix using the 'funct.dist' function, which is based on Gower's distance (Gower, 1971) and adapted from the 'gawdis' function (de Bello et al., 2020). This allows for the treatment of multiple variable types (e.g. ordinal and nominal; Table S1; supplementary methods), to give different weights to each dental character (see below), and to retrieve the axes of a principal coordinate analysis (herein, PCoA; Magneville et al., 2022). Given that the associations between dental characters and functional traits are not always one-to-one, we assigned weights to some dental characters to avoid the overrepresentation of some aspects of tooth morphology and therefore, functional traits (de Bello et al., 2020; Pavoine et al., 2009). Accordingly, we assigned a weight of 0.5 to crown height and to crown width, as both are tooth-size characters and proxies for body size (Table S2; Cooper et al., 2023 and references therein). We further weighted cross-section outline and longitudinal outline at 0.33 and 0.67, respectively, as both are tooth-shape-related characters and proxies for feeding mechanism, with longitudinal outline being a more important proxy (Table S2; Cooper et al., 2023). The remaining dental characters (i.e. cutting edge and lateral cusplets) were assigned weights of one each, as they are independently associated with prey preference and feeding mechanism respectively (Cooper et al., 2023).

Using the 'quality.fspaces' function, we determined that our data were best represented in four dimensions (Figure S2; Maire et al., 2015). However, we built our space using three dimensions because (1) the difference in mean absolute deviation values between a three- and four-dimensional space was negligible (<0.0001; Figure S2); and (2) 78.4% of the total inertia was represented within the first three axes. Based on the functional space built using all taxa, we assessed the relationship between axes and dental characters (Table S4; Figure S3) using the 'traits.faxes.cor' function. To test the effect of our dental character weightings on these relationships, we repeated the above steps without weighting dental characters (Table S4). We used the 'alpha.fd.multidim' function to calculate functional richness (FRic; % volume of the functional space occupied), mean originality (FOri; the distance of each taxa to its closest neighbour) and mean specialization (FSpe; the distance of each taxa to the functional space centroid) per time bin. We also calculated the FRic and mean FOri and FSpe of extinct and extant taxa and the mean FOri and FSpe across shark orders. Finally, we used the "fuse" function to compute species' individual FOri and FSpe (Griffin et al., 2020; Pimiento et al., 2020) and ranked taxa according to their scores to identify the top 5% contributors.

For all metrics described above, we reported the median and standard deviation (SD) per time bin, as the data across FTU iterations were not normally distributed (Shapiro–Wilk; $p < 0.05$). Based on median values, we plotted the functional space of the entire Cenozoic assemblage and identified its vertices using the functions 'background.plot' and 'vertices' respectively. We also built the functional spaces of each time bin and of extinct and extant taxa using the 'alpha.multidim.plot' function. We additionally used Mann–Whitney U-tests to assess whether the differences across epochs (i.e. assessed in pairwise time bins) were statistically significant. Furthermore, we performed a Welch two sample *t*-test to assess whether mean FOri and FSpe values of extinct and extant taxa were statistically different, and two-sided 90th quantile permutation tests ($n = 5000$; Cooke et al., 2022) to assess if outliers in FSpe or FOri distributions of the extinct or extant samples deviated due to random chance.

2.2.4 | Assessment of sampling biases

First, we assessed how sampling biases might affect the number of taxa recorded in each time bin (i.e. empirical taxonomic richness), and consequently the functional diversity metrics. To do so, we randomly resampled each time bin based on the lowest sample size in our dataset (Pleistocene = 309 teeth) using the 'sample' R function and re-calculated the number of taxa as well as all functional diversity metrics per time bin 1000 times without replacement. We also assessed whether changes in the empirical number of taxa through time were statistically different from those seen when taxonomic richness was resampled. We did this by (1) calculating the net-changes of taxonomic richness between successive time bins in both the empirical and resampled data; (2) subtracting the empirical net-changes from their resampled counterparts to find the difference in net-changes between the two samples, done for all 1000 resampled iterations (see above); (3) bootstrapping the resampled net-changes to obtain a median of differences per net-change and assessing the central tendency and uncertainty with confidence interval tests and (4) performing a one-tailed bootstrap hypothesis test per net-change to determine if the returned differences were statistically significant.

We also assessed how the degradation of our Recent sample (i.e. including only extant taxa with a fossil record) affected our results. To do so, we re-calculated FRic (i.e. % volume of the functional space occupied) for (1) all taxa from the present-day (i.e. herein 'Recent-plus', which includes taxa without a fossil record; $n = 162$); and (2) a random subsample of the 'Recent-plus' based on the number of taxa with a fossil record (i.e. herein 'Resampled Recent-plus'; $n = 114$) 1000 times without replacement. We compared these values against those from the degraded Recent sample.

Finally, we performed a complementary analysis (see supplementary methods) to assess (1) how much of a functional space comprising the total diversity of living sharks is represented by our degraded Recent sample; and (2) whether the degraded Recent sample is missing the most extreme trait values from today's diversity. To do this, we collected trait data of all living species based on the literature (Data S2). Specifically, we collected data on the traits that our dental characters serve as proxies of (i.e. body size, prey preference and feeding mechanism; Cooper et al., 2023). Body size and prey preference were obtained from Pimiento et al. (2023), whereas feeding mechanism was obtained from Kent (1994, 2018) and Cappetta (2012).

2.2.5 | Null model

We compared all functional diversity metrics per time bin against a null model to examine whether our results differ from random expectations based on empirical taxonomic richness. Accordingly, for each time bin, we randomized taxonomic identity while maintaining the empirical number of taxa and re-calculated all functional diversity metrics 1000 times. To compare the median values from this null model against those obtained empirically we used *Z*-scores (i.e. [empirical median − null model median]/null model SD). *Z*-scores with an absolute value of $>|1.96|$ were considered statistically significant and indicative of empirical results falling beyond 95% of the null distribution (Hedberg et al., 2021).

2.2.6 | Sensitivity analyses

To assess the sensitivity of our functional diversity analyses to individual traits (Lefcheck et al., 2015), we computed all functional diversity metrics described above, but removing one dental character at a time.

2.2.7 | Random simulations of species loss

We examined how changes in FRic over time differ from expectations based on a random simulation of taxonomic loss. Accordingly, we computed FRic in randomized subsamples sequentially going from 10 to the total number of taxa (537), 100 times without replacement (Pimiento et al., 2020). This procedure allowed us to establish the expected relationship between FRic and taxonomic richness and assess deviations from expectations.

3 | RESULTS AND DISCUSSION

3.1 | Structure of Cenozoic shark functional space

Our PCoA based on dental measurements (trait-proxies) revealed that the Cenozoic shark assemblage can be represented within a reduced three-dimensional trait space (representing 78.4% of the total inertia; Figures 1a and S2). The first axis (50.5% inertia) was most correlated to lateral cusplets and longitudinal outline (Table S4), which, based on Cooper et al. (2023), are associated with feeding mechanism (Table S2). Although these dental characters were weighted at one and 0.67 respectively (see Methods), they were also found to be the most correlated to PCoA1 when unweighted (Table S4). An extinct megamouth shark, †*Megachasma alisonae*, scored the lowest value along this axis (Figure 1a), with teeth displaying the presence of lateral cusplets and piercing longitudinal outlines, representing clutching and vestigial feeding mechanisms (Cooper et al., 2023). Such inferences broadly agree with literature, where †*M. alisonae* has been interpreted as

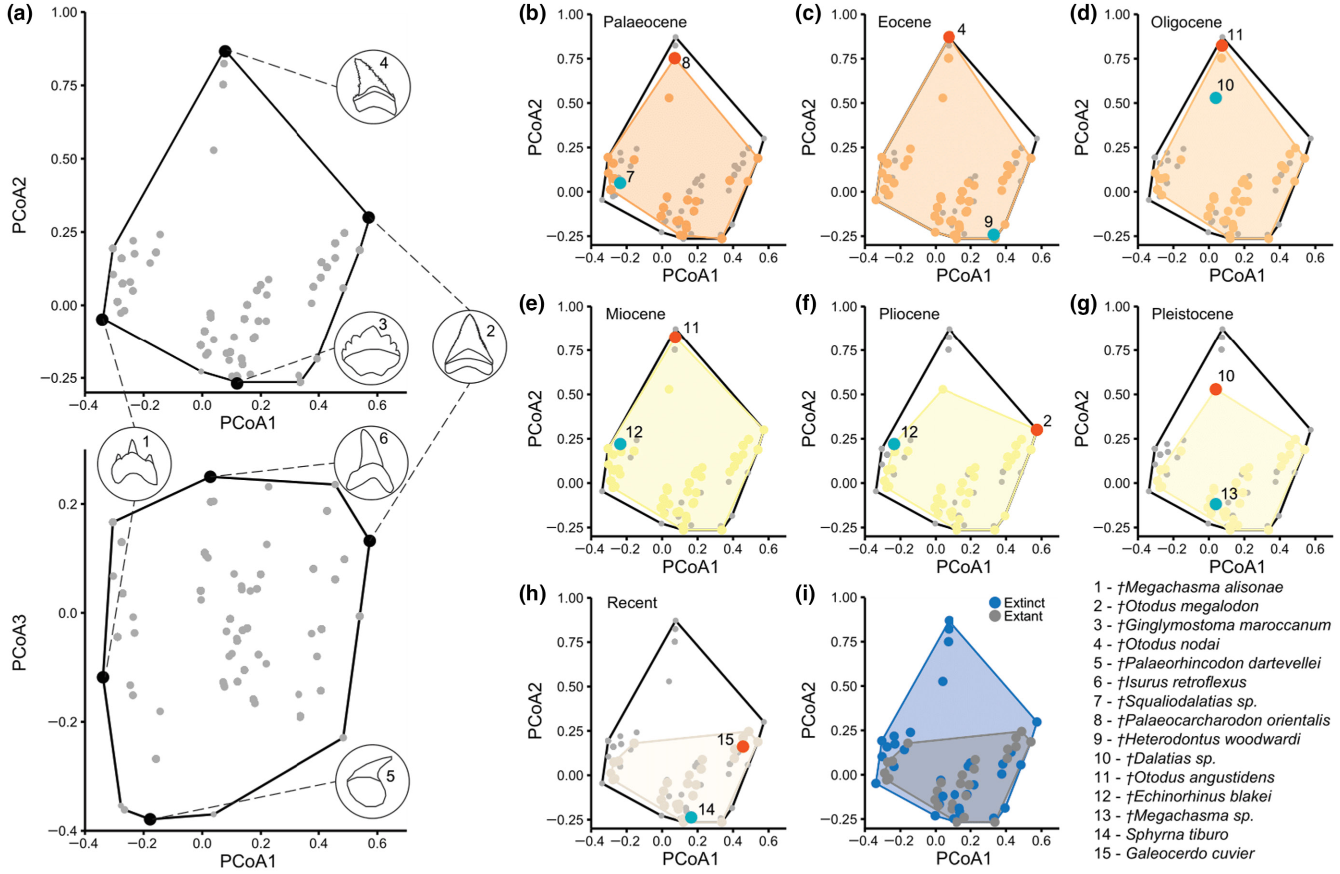

FIGURE 1 Functional space of Cenozoic sharks. (a) Structure of the three-dimensional functional space for all sharks. Black dots represent the highest and lowest scoring taxon per axis, with their corresponding teeth illustrated and numbered following an accompanying legend. Grey dots mark all other taxa. (b–h) Shark functional spaces over time (only two dimensions shown here; see Figure S4), with space occupied in each time bin depicted by coloured convex hulls. Note that the Holocene was excluded from our analyses (see text). Coloured dots denote taxa present in each assemblage, while grey dots represent absent taxa. Turquoise and orange dots denote taxa with the highest FOri and FSpe scores, respectively, which are detailed in the legend. (i) Convex hulls of extinct (blue) and extant (grey) sharks.

a filter feeder (Shimada & Ward, 2016). The highest value along this axis was scored by the extinct 'megalodon' †*Otodus megalodon* (Figure 1a), whose teeth lack lateral cusplets and had triangular longitudinal outlines, representing a cutting feeding mechanism (Cooper et al., 2023). Indeed, †*O. megalodon* likely fed by slicing large prey (Cappetta, 2012; Kent, 1994).

The second axis (19.5% inertia) was most correlated with cutting edge and crown height (Table S4), which collectively relate mainly to prey preference (Table S2; Cooper et al., 2023). The lowest scoring species was an extinct nurse shark †*Ginglymostoma maroccanum* (Figure 1a), with teeth displaying smooth cutting edges and small crown heights, broadly indicating a preference for invertebrates, in line with the ecology of its extant relatives (Cooper et al., 2023; Ebert et al., 2021). The highest scoring species was †*Otodus nodai* (Figure 1a), an extinct megatoothed shark possessing teeth with serrated cutting edges and large crown heights, suggesting a prey preference for high vertebrates (e.g. seabirds and marine mammals; Cooper et al., 2023; Cortés, 1999). Interestingly, the highest values along PCoA2 were largely unoccupied (Figure 1a), suggesting that some possible forms of shark tooth morphology were not realized. Indeed, only 5.65% of all possible dental character combinations were filled (see Methods). The highest scoring values along this axis represent the tooth morphology of top predators (i.e. the largest teeth with serrated edges; Cooper et al., 2023). The empty space along PCoA2 could be due to the fact that top predatory traits are rare in ecosystems because large body sizes and specialized diets result in low energy efficiency and population abundance (Garcia et al., 2008; Munroe et al., 2013). Therefore, large top predators are functionally distinct compared to smaller, more generalist sharks, which is reflected in their extreme and/or solitary positions in trait space.

The third axis (8.4% inertia) of the functional space was most correlated with crown height (Table S4), which is strongly related to body size and prey preference (Table S2; Cooper et al., 2023). The lowest scoring species was an extinct whale shark †*Palaeorhincodon dartevellei*, which is inferred to have been planktivorous based on its small teeth (Kent, 1994). An extinct mako shark, †*Isurus retroflexus*, scored the highest value (Figure 1a), which is inferred to have fed on large fishes based on its large teeth and extant counterparts (Cooper et al., 2023; Ebert et al., 2021). Interestingly, the species scoring the highest and lowest values along PCoA3 do not display contrasting body sizes. Indeed, planktivorous species can reach large sizes despite their small teeth, with the extant whale shark *Rhincodon typus*, reaching up to 21 m in total length (Ebert et al., 2021). Therefore, PCoA3 appears to largely display variation in prey size, rather than body size.

Overall, examining the Cenozoic shark functional space (Figures 1 and S4) revealed that low values of the trait-space were occupied by teeth broadly associated with benthic feeding ecology (i.e. small, smooth and piercing or semi-circular teeth indicating sharks feeding on small prey such as invertebrates via clutching and vestigial mechanisms), whereas high values were occupied by teeth associated with high-level macropredators (i.e. large, serrated and triangular teeth reflecting cutting mechanisms and a prey preference for large prey such as high vertebrates).

3.2 | How has functional diversity of sharks changed through time?

The number of collected taxa (i.e. empirical sample) was lowest in the Palaeocene, at the beginning of the Cenozoic (Figure S5a). This number more than doubled in the Eocene, where maximum richness was reached, marking the largest increase in taxonomic diversity in the Cenozoic based on our sample. Sampled taxa subsequently dropped by 55% in the Oligocene, which represents the largest taxonomic decline observed, followed by a 93% increase in the Miocene. Thereafter, the number of collected taxa decreased in the Pliocene, Pleistocene and Recent, by 37%, 9% and 15% respectively (Figure S5a). When accounting for uneven sampling based on our resampling procedure (see Methods), we found the same general pattern (Figure S5). However, we also found small differences, including an almost negligible (3%) increase from the Pliocene to the Pleistocene (as opposed to a 9% decrease), and that the Recent (and not the Palaeocene) was the time bin with the lowest taxonomic richness (empirical Palaeocene = 105, Recent = 114; resampled Palaeocene = 87, Recent = 83; Figure S5). Nevertheless, the results found using the empirical data provide a useful representation of the changes in taxonomic richness throughout the last ~66 million years (Myr) given that: (1) the differences in the general pattern of taxonomic richness over time were small; and (2) the difference in net-change between empirical and resampled data displayed small uncertainty (i.e. a range within ±1 of the central tendency for all net-changes) and were not statistically significant ($p > 0.05$; Table S5).

3.2.1 | Palaeocene

Our FE approach showed that the Palaeocene epoch (66–56 Ma) had the lowest FE richness and FRed of the Cenozoic (Table 1; Figure 2a,b), specifically during the early and middle Palaeocene respectively (i.e. Danian-Selandian, 66–59.2 Ma; Figure S6a,b). The functional space approach further revealed that Palaeocene sharks spanned over half of the functional space (FRic = 66%; Table 1; Figures 1b and 2d). Relatively high FOri and FSpe values compared to the rest of the Cenozoic were established in the Palaeocene; however, these values only marginally changed thereafter at the epoch level (Table 1; Figure 2e,f). At the stage level, FOri displayed the highest values in the middle Palaeocene (Selandian, ~60 Ma; Table 1; Figure S6e). Of all the functional diversity metrics considered, FOred and FRic significantly differed from the null model (i.e. where we randomized species identities while maintaining the empirical taxonomic richness; see violin plots in Figure 2), with values, respectively, 6% and 23% higher than expected in the Palaeocene (Tables 2 and S6), and 6% and 19% higher than expected in the Danian and Selandian respectively (~63.5 Ma and ~60 Ma; Tables S7–S9). These results suggest that although the Palaeocene was poor in terms of number of ecological functions and redundancy, it displayed a considerably wide range of different functions, more so than expected. Indeed, examining FRic changes in response to taxonomic richness showed that FRic approaches 50% on average with as few as 70 taxa

TABLE 1 Diversity metrics per time bin ("Epoch").

Epoch	Time (Ma)	FEs	FRed	FOred (%)	FRic (%)	FOri	FSpe
Palaeocene	66–56	32	3.25	48	66	0.022	0.308
Eocene	56–33.9	55 **(+72%)**	4.82* (+48%)	50* (+2%)	86 **(+20%)**	0.016 (−27%)	0.304 (−1%)
Oligocene	33.9–23.03	43 (−22%)	2.67 (−45%)	40 (−10%)	78 (−8%)	0.021 **(+31%)**	0.300 (−1%)
Miocene	23.03–5.33	56* (+30%)	4.18 **(+56%)**	46 **(+6%)**	87* (+9%)	0.020 (−5%)	0.302 (+1%)
Pliocene	5.33–2.58	49 (−12%)	2.92 (−30%)	41 (−5%)	69 (−18%)	0.024* (+20%)	0.309* **(+2%)**
Pleistocene	2.58–0.01	44 (−10%)	3.02 (+4%)	42 (+1%)	60 (−9%)	0.020 (−17%)	0.302 (−2%)
Recent	0	36 (−18%)	3.17 (+5%)	43 (+1%)	43 (−17%)	0.012 (−40%)	0.293 (−3%)

Note: Functional diversity metric values are medians calculated from 1000 iterations of empirical analyses, accurate to three decimal places for FOri and FSpe, and up to two for all other metrics. Proportional changes from one epoch to the other are in parentheses, calculated based on values within the table. Bold denotes largest proportional changes (black, increases; grey, decreases). Asterisks denote highest values per metric.

Abbreviations: FEs, number of functional entities; FOred, functional over-redundancy (% of species filling entities above mean level FRed); FOri, functional originality (mean distance of taxa to their closest neighbour); FRed, functional redundancy (average number of species per FE); FRic, functional richness (% of space volume occupied); FSpe, functional specialization (mean distance of species to the centroid of the space); Ma, million years ago.

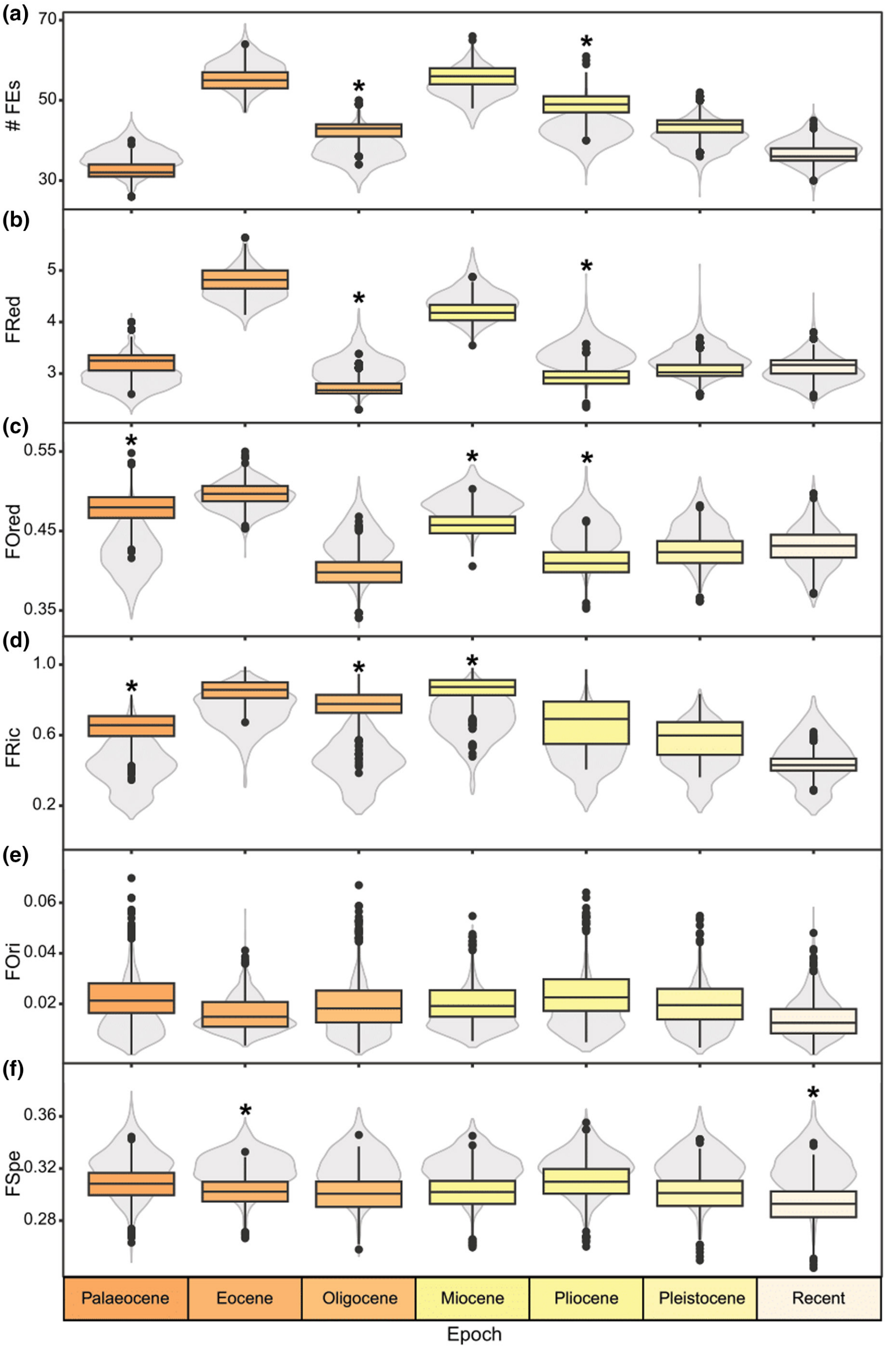

FIGURE 2 Changes in shark functional diversity through time. (a) number of functional entities (# FEs); (b) functional redundancy (FRed); (c) functional over-redundancy (FOred); (d) functional richness (FRic); (e) functional originality (FOri) and (f) functional specialization (FSpe). Boxplots showcase values across 1000 iterations in which random dental character combinations (i.e. FTUs; see Methods) were selected per taxon to account for intraspecific variation. Grey violin plots display the range of values from the null model across 1000 iterations. See Table 1 for all values per time bin. Asterisks denote significant deviations from null expectations.

(Figure S7), suggesting that even species-poor shark assemblages can have a broad range of functions in the Cenozoic.

The Palaeocene represents the aftermath of the Cretaceous-Palaeogene (K/Pg) mass extinction, in which elasmobranchs lost at least 60% of their diversity, with durophagous sharks (those eating shelled invertebrates) being the most affected (Guinot & Condamine, 2023; Kriwet & Benton, 2004). This depletion of species diversity likely explains the low FE richness of this epoch. Moreover, the K/Pg extinction particularly diminished large-bodied teleosts (Friedman & Sallan, 2012), suggesting that shark prey may have been somewhat limited, potentially resulting in functional redundancy being packed into few FEs (i.e. higher than expected FOred). However, during this time, ocean temperature and eustatic sea level increased (Miller et al., 2005; Zachos et al., 2001), and ray-finned fishes diversified and became highly abundant, taking advantage of the vacant niches left after the K/Pg (Alfaro et al., 2018; Sibert & Norris, 2015). As such, the higher-than-expected range of ecological functions (i.e. FRic) of the Palaeocene could be linked to the highly productive and extensive coastal habitats of the time (e.g. Pimiento et al., 2017), and to the availability of prey for piscivore diets.

3.2.2 | Eocene

The Eocene (56–33.9 Ma) showcased a marked increase in FE richness and FRed, the latter reaching its highest Cenozoic value during

TABLE 2 *Z*-scores for all functional diversity metrics calculated, indicating how the empirical result of each metric differs from random chance expectations based on the number of taxa.

Epoch	FE	FRed	FOred	Fric	FOri	FSpe
Palaeocene	−1.81	1.89	**3.33**	**2.91**	1.14	−1.06
Eocene	−0.91	0.88	0.36	1.60	0.16	**−1.98**
Oligocene	**2.59**	**−2.41**	−1.87	**4.12**	0.67	−1.67
Miocene	1.10	−0.95	**−2.25**	**2.38**	1.00	−1.77
Pliocene	**3.28**	**−2.98**	**−2.46**	1.66	1.37	−0.89
Pleistocene	1.43	−1.30	−1.07	0.99	0.82	−1.62
Recent	−0.74	0.75	0.18	−0.30	−0.34	**−2.24**

Note: All values are accurate to two decimal places. *Z*-scores marked in bold are considered statistically significant ($Z > |1.96|$), marking a value that falls outside of 95% of the null distribution.

Abbreviations: FE, functional entities; FOred, functional over-redundancy; FOri, functional originality; FRed, functional redundancy; FRic, functional richness; FSpe, functional specialization.

this time (Table 1; Figure 2), specifically during the middle Eocene (Lutetian; ~45 Ma; Figure S6b; Table S7). FRic also expanded, reaching near-maximum levels (Table 1; Figures 1c and 2d), specifically in the late Eocene (Priabonian; ~35 Ma; Figure S6d; Table S7). FE richness, FRed and FSpe slightly deviated from null expectations, with FSpe being 5% lower than expected for the Eocene (Tables 2 and S6) and FE richness and FRed being 12% higher and 11% lower, respectively, than null expectations for the Priabonian (Figure S6; Tables S8 and S9). Together, these results indicate a significant rise in shark functional diversity during the Eocene, as indicated by the increase in FEs and FRic. Taxa were also slightly less specialized than expected which, together with the high levels of functional redundancy (maximum FRed), likely conferred the Eocene assemblage some level of ecological insurance.

The Eocene marked the warmest epoch in the Cenozoic (Zachos et al., 2001), which has been linked to increased productivity (Rabosky & Sorhannus, 2009) and the emergence of marine mammals (Uhen, 2007). These environmental and biotic changes likely enhanced habitat complexity and expanded prey availability for sharks (Ciampaglio et al., 2005), which may have, in turn, enabled the emergence of new ecological functions and facilitated functional space expansion (i.e. increasing FEs and FRic; Table 1). Indeed, it is during the Eocene that sharks feeding on high vertebrates start occupying the highest scores along PCoA2 (Figure 1c). Moreover, invertebrates and fishes—prey already available to sharks prior to this epoch—continued to diversify during the Eocene (Alroy et al., 2008; Guinot & Cavin, 2016), potentially allowing functional redundancy to consolidate (i.e. peak FRed; decreasing FOri and FSpe; Table 1).

3.2.3 | Oligocene

The Oligocene (33.9–23.03 Ma) experienced the largest declines of FE richness, FRed and FOred, the latter two hitting their lowest values of the Cenozoic at the epoch level (Table 1; Figure 2a–c). Despite these changes, FRic declined only by 8% (Table 1; Figures 1d and 2d), largely retaining the Eocene functional space, even at stage level (Figure S6d; Table S7). Meanwhile, FOri underwent its largest increase, signifying increased taxon isolation in trait space (Table 1; Figure 2e). Of all metrics, FE richness, FRed, FRic and FOred significantly deviated from null expectations (Tables 2 and S9). Specifically, FE richness and FRic were, respectively, 16% and 32% higher than expected, while FRed was 14% lower than expected (Tables 2 and S6). Similar deviations were also found in both Oligocene stages, though the FRic deviation was restricted to the early Oligocene (Rupelian; ~30 Ma), and FOred was 5% lower than expected only at the stage level (Figure S6a–d; Table S8). Our results indicate that although the Oligocene shark assemblage experienced important redundancy losses (Table 1; Figure 2), there was not a significant reduction of ecological functions, as indicated by the FE and FRic values, which were higher than expected. Indeed, the relationship between FRic and taxonomic richness becomes more asymptotic as FRic approaches 80% (Figure S7). Interestingly, these changes in functional diversity did not result in the overrepresentation of some FEs, as indicated by the low FOred values (Figures 2 and S6c), which were significantly lower than expected at stage level (Tables S8 and S9). The relative resilience of functional diversity during the Oligocene was likely the result of the ecological insurance reached during the Eocene. Nevertheless, functional redundancy was largely depleted during the Oligocene, as evidenced by the increase in FOri and decrease in FRed, the latter being lower than expected based on taxon numbers (Figure 2; Table 2). Overall, our results collectively suggest that the Oligocene shark functional diversity was somewhat buffered by the ecological redundancy reached in the Eocene, but the loss of this redundancy in the Oligocene (Figure S6), likely left the assemblage highly vulnerable.

During most of the Oligocene, the oceans were cooler than in the Eocene (Zachos et al., 2001), likely resulting in a decline in eustatic sea level (De Boer et al., 2010; Miller et al., 2005). These changes may have led to a reduction in the extent of coastal habitats for sharks and their prey (e.g. Pimiento et al., 2017) which could be linked to the declines in functional diversity (i.e. 22% decline in FE richness and 45% decline in FRed). However, the continued diversification of fishes and marine mammals during this time (Guinot & Cavin, 2016; Uhen, 2007) may have ensured access to diverse prey, as evidenced by the lower-than-expected functional losses and the maintenance of most of the extent of functional space.

3.2.4 | Miocene

In the Miocene (23.03–5.33 Ma), shark functional diversity displayed marked recoveries from the Oligocene: FE richness and FRic reached the maximum values of the Cenozoic (Table 1; Figures 1e and 2a–d), with FRic being 17% higher than expected (Tables 2 and S6). These peaks in functional diversity were specifically observed in the early and middle Miocene (FEs peak in the Aquitanian-Burdigalian, 23.03–15.97 Ma; FRic peaks in the Aquitanian-Serravallian, 23.03–11.63 Ma; Figure S6; Table S7). In the late Miocene (Tortonian and Messinian; 11.63–5.333 Ma), however, shark functional diversity declined, as evidenced by a decrease in FEs and FRic (Figure S6; Table S7). Miocene functional redundancy metrics did not experience the same level of recovery as other functional diversity metrics. Although FRed increased from the Oligocene to the Miocene, values were lower than expected throughout most Miocene stages (Figure S6; Tables S8 and S9). Similarly, FOred increased in the Miocene, despite being lower than expected (Figures 2 and S6; Tables 2 and S9). When taken together, our results suggest that although shark assemblages exploited the maximum range of ecological functions in the early and middle Miocene, they did not necessarily increase their ecological resilience due to their lower-than expected functional redundancy and high over-redundancy (Figure S6; Tables S7–S9).

The Miocene epoch was a time of large environmental and biological changes. Temperatures were relatively high throughout the early and middle Miocene (Zachos et al., 2001), resulting in increased eustatic sea level (De Boer et al., 2010) and ocean productivity (Marx & Uhen, 2010). Consequently, cetaceans diversified, reaching their highest diversity in the Tortonian (lower late Miocene; ~10 Ma; Marx & Uhen, 2010). Although these conditions became volatile from the late Miocene onwards, overall, the first half of the Miocene provided sharks warm temperatures and, importantly, diverse, large prey. These favourable conditions likely enabled the larger-than-expected expansion of the functional space, with the Miocene being the epoch with the largest space occupation of the entire Cenozoic, (i.e. FRic = 87%; Table 1). Some of this expansion was driven by the appearance of new, highly specialized species, specifically, the largest macropredatory shark that has ever lived, †*O. megalodon*, which likely preyed upon marine mammals (e.g. Collareta et al., 2017; Godfrey et al., 2021; Godfrey & Beatty, 2022) and sits at the extreme of PCoA1 (Figure 1a,e).

3.2.5 | Pliocene

Pliocene (5.33–2.58 Ma) sharks experienced dwindling FE richness, FRed, FOred and FRic relative to the Miocene (Tables 1 and S7; Figures 1f, 2a–d, and S6). Notably, Pliocene sharks experienced the highest loss of functional space of the entire Cenozoic (i.e. 18% loss; Table 1). Moreover, taxa became more isolated in and occupied extreme positions of the trait space, as denoted by rising FOri and FSpe, which reached their maximum Cenozoic values (Tables 1 and S7; Figures 2 and S6). From these metrics, FE richness, FRed and FOred exceeded null expectations (Table 2). FE richness was 17% higher than expected, while FRed and FOred were, respectively, 14% and 4% lower than expected (Tables 2, S6–S9; Figure S6a–c). Together, these results suggest that the number of shark ecological functions (FEs) and functional redundancy (FRed) diminished in the Pliocene, with taxa becoming more functionally specialized than in any other time bin (Table 1; Figure 2f). Despite these changes being less dramatic than expected, the Pliocene assemblage was likely highly vulnerable to further losses.

From the late Miocene and throughout the Pliocene, ocean temperature, productivity, eustatic sea levels and the extent of coastal habitats underwent significant fluctuations, with an overall trend of decline (De Boer et al., 2010; Marx & Uhen, 2010; Miller et al., 2005; Pimiento et al., 2017; Zachos et al., 2001). Cetacean diversity largely mirrored this trend, with an initial increase in the early Pliocene (Zanclean; ~4.5 Ma) and a dramatic decrease towards the late Pliocene (Piacenzian; ~3 Ma; Marx & Uhen, 2010, Pimiento et al., 2017). These changing conditions likely resulted in limited prey availability for sharks, potentially explaining the loss of functional diversity observed in the Pliocene, specifically the contraction of trait space along PCoA2 (Figure 1f), which is mostly related to a prey preference for high vertebrates (Table S2).

3.2.6 | Pleistocene

In the Pleistocene (2.58–0.01 Ma), FE richness and FRic continued to decline from the Pliocene, while FRed and FOred maintained Pliocene levels (Table 1; Figures 1g and 2). All functional diversity metrics maintained similar values throughout all stages of the Pleistocene (Figure S6; Table S7). Moreover, no metric deviated from null expectations at either epoch or stage level (Tables 2 and S9). Overall, these results suggest that the Pleistocene shark functional diversity represents a continuation from the Pliocene assemblage, with functional diversity remaining as expected given the losses from the previous epoch.

The Pleistocene oceans experienced violent temperature and sea level oscillations (De Boer et al., 2010; Miller et al., 2005; Zachos et al., 2001), which resulted in ample fluctuations of neritic area available, and ultimately, a significant decrease in the extent of productive coastal habitats (Pimiento et al., 2017). It has been proposed that these area changes were key drivers in the extinction of one-third of the marine megafauna in the Plio-Pleistocene transition, which mostly affected homeothermic animals, including mesothermic sharks (Pimiento et al., 2017). Indeed, the giant macropredator †*O. megalodon* became extinct during this event, specifically in the late Pliocene (Boessenecker et al., 2019; Pimiento & Clements, 2014). Although most of the functional space had already been lost by the Pliocene, the extinction of †*O. megalodon* resulted in further loss of trait space, particularly along PCoA1 and PCoA2, which, combined, represent the ecological role of a super predator (Cooper et al., 2022; Kast et al., 2022).

3.2.7 | Recent

In the Recent sample, FE richness continued to decrease, while FRed and FOred largely retained Pleistocene values (Table 1; Figure 2a–c). Meanwhile, FRic, FOri and FSpe reached their lowest Cenozoic values (Table 1; Figures 1h, 2e,f, and S6d; Table S7). FSpe and FRic were the only metrics significantly deviating from null expectations, FSpe at the epoch level (Tables 2 and S6) and FRic at the stage level (Figure S6; Table S9). Our sampling bias assessments revealed that the FRic decline in the Recent is not likely to be a sampling artefact. Specifically, when assessing whether our findings are the result of our degradation of the Recent (see Methods), we found that the inclusion of present-day species without a fossil record (i.e. the 'Recent-plus' sample) does not extend the space occupied in this time bin (Figure S8), nor does it when resampling the 'Recent-plus' based on the degraded Recent sample size ('resampled Recent-plus'; Figure S8). Indeed, the 'Recent-plus' FRic was significantly lower than expected ($Z = -4.56$; Figure S8). As such, the FRic found based on empirical data is a conservative estimate. Furthermore, when assessing the space occupied by the degraded Recent sample in a functional space built using the total extant diversity (see Methods), we found that the degraded Recent sample occupies 98% of the modern functional space and includes the most functionally specialized living species (Figure S9). This indicates that our Recent sample largely captures the extent of ecological functions of modern sharks. Finally, the decline in FRic in the Recent was significantly different than expected based on random taxonomic loss (Figure S7). Indeed, the loss of taxa from the Pleistocene to the Recent was expected to approach Palaeocene values based on simulations of randomized taxonomic loss (FRic = ~60%; Figure S7), instead of the values found empirically (FRic = 43%; Figures 2 and S6).

Taken together, our results suggest that although shark taxa are less isolated in trait space in the Recent than in the Pleistocene (i.e. decreased FOri and FSpe), the Recent sample occupied less than half of the Cenozoic functional space (FRic = 43%), a level of FRic not even seen in the Palaeocene after the K/Pg extinction (Figure 1; Table 1), which is a conservative estimate based on our tests (see above). As such, shark functional diversity is potentially depleted today compared with the last ~66 Myr. Considering the losses of shark functional diversity since the late Miocene, this level of ecological loss appears to be the continuation of a long-term decline (Figures 1f–h and 2). Nevertheless, the extent of functional space of the Recent is markedly diminished compared with the Pleistocene, especially along PCoA2. This erosion of functional space resulted from the loss of †*Dalatias* sp. an extinct form of kitefin shark, which represents the ecological role of deep-water species potentially specialized in preying upon large fish (Navarro et al., 2014). Although the functional space of the Recent sample provides a useful comparison with the geological past and with modern assemblages (see Methods and above), it is still a subsample of the current shark functional diversity. Nevertheless, when examining vertices of the Recent functional space, we can identify the species holding the extremes of the functional volume still preserved from the geological past. These include the bluntnose sixgill shark (*Hexanchus griseus*; IUCN Red List status = Near Threatened) and the Iceland catshark (*Apristurus laurussonii*; IUCN = Least Concern), which preserve the remains of the highest and lowest values along the Cenozoic PCoA1. Similarly, the horn shark (*Heterodontus francisci*; IUCN = Data Deficient) and the great white shark (*Carcharodon carcharias*; IUCN = Vulnerable) preserve the lowest and highest ends along the Cenozoic PCoA2. Finally, the tiger shark (*Galeocerdo cuvier*; IUCN = Near Threatened) and the short-tail nurse shark (*Pseudoginglymostoma brevicaudatum*: IUCN = Critically Endangered; IUCN, 2023) preserve the extreme portions of the Cenozoic functional space along PCoA3 (Figure S10). The protection of these species could potentially complement current recommendations for the conservation shark functional diversity (Pimiento et al., 2023).

3.2.8 | The rise and fall

Collectively, our tooth-based analyses revealed that shark functional diversity was generally high in the Cenozoic past (i.e. FRic = 60%–87%) compared with the Recent (i.e. FRic = 43%). This diversity experienced fluctuations through time, with peaks in the Eocene and Miocene (Table 1; Figures 1 and 2), and a steady decline from the late Miocene onwards. All functional diversity changes over time were significantly different across consecutive time bins, as evidenced by pairwise statistical comparisons (Mann–Whitney U-tests; $p \leq 0.01$; Table S10). Our results are robust in the face of sampling artefacts, different trait treatments and uneven time bin durations. Specifically, our functional diversity estimates do not appear to be affected by uneven sampling (Figure S5), or by the removal of individual traits (Figure S11), and were upheld when analysed at the stage level (Figure S6). Lastly, our estimates of Recent FRic appear to be largely conservative and capture the extent of functions of the modern assemblage (Figures S8 and S9).

Our study does not allow us to establish the causal mechanisms behind the observed changes in functional diversity. However, fluctuations in global temperature, productivity, sea level and prey availability largely coincide with the rise and fall of shark functional diversity. Despite the environmental fluctuations of the Cenozoic era, the overall trend of the last ~66 Myr has been of cooling (Burke et al., 2018; Zachos et al., 2001). Today, however, modern shark communities are encountering markedly different conditions, with ocean temperatures rapidly increasing due to human-produced greenhouse gas emissions (Smith et al., 2015). Future projections suggest that under unmitigated scenarios, temperatures by the year 2150 could resemble those of the Eocene epoch, potentially reversing a 50-million-year cooling trend in less than 200 years (Burke et al., 2018). Although we found that functional diversity peaks coincided with global warming events in the geological past, studies indicate that modern sharks are being adversely affected by anthropogenic global warming and ocean acidification (Rummer et al., 2022). Specifically, critical habitats for shark survival, such as coral reefs and nursery areas are diminishing, and shark native ranges are becoming less suitable (Coulon et al., 2024; Dulvy et al., 2021). Nevertheless, these oceanographic changes are not the primary threat to sharks today; instead, overfishing is directly driving around 40% of living shark species towards extinction (Dulvy et al., 2021; Pimiento et al., 2023). Understanding the mechanisms shaping shark functional diversity across evolutionary timescales requires careful consideration of multiple confounding factors and their interactions, presenting a promising avenue for future research.

3.3 | Which species had the largest contributions to functional diversity?

3.3.1 | Extinct versus extant

We found no clear difference between mean functional originality (FOri) and specialization (FSpe) of extinct versus extant sharks (Welch two sample *t*-test; FOri: $t=0.046$, df = 208.01, $p=0.96$; FSpe: $t=-0.9$, df = 212.81, $p=0.37$; Figure 3a,c). However, there were several high-scoring outliers in the FSpe distribution, almost all of which are extinct (Figure 3c). Moreover, these outliers were not found to deviate from the FSpe distribution by chance (Two-sided 90th quantile permutation tests; $p=0.016$, see Methods). As such, extinct sharks spanned a considerably wider range of the functional space (FRic = 98.7%) than extant sharks (FRic = 43%; Figures 1i and S4a). Indeed, the highest and lowest scoring species of all three functional axes were extinct (Figure 1a).

Ranking the top 5% FOri and FSpe taxa further revealed that most of these taxa were extinct (Figure 3b,d). This included the top six FOri and the top 20 FSpe taxa. Interestingly, seven of the top 10 FSpe taxa (Figure 3d) belonged to a single genus: †*Otodus* (i.e. the 'megatoothed' sharks), a clade well known for their gigantic body sizes (8–20 m long) and high trophic levels (Cooper et al., 2022, Kast et al., 2022). It can thus be inferred that the †*Otodus* clade performed a specialized ecological function during the Cenozoic; a function that would have been lost in the Pliocene following the extinction of its last surviving species, †*O. megalodon* (Boessenecker et al., 2019; Kast et al., 2022; Pimiento et al., 2016; Pimiento & Clements, 2014). Together, our results indicate that extinct species disproportionally contributed to Cenozoic shark functional diversity, more so than their extant counterparts (Figures 1i and 3), largely explaining the diminishing of functional diversity in the Recent when compared to the past (Figures 2 and S6).

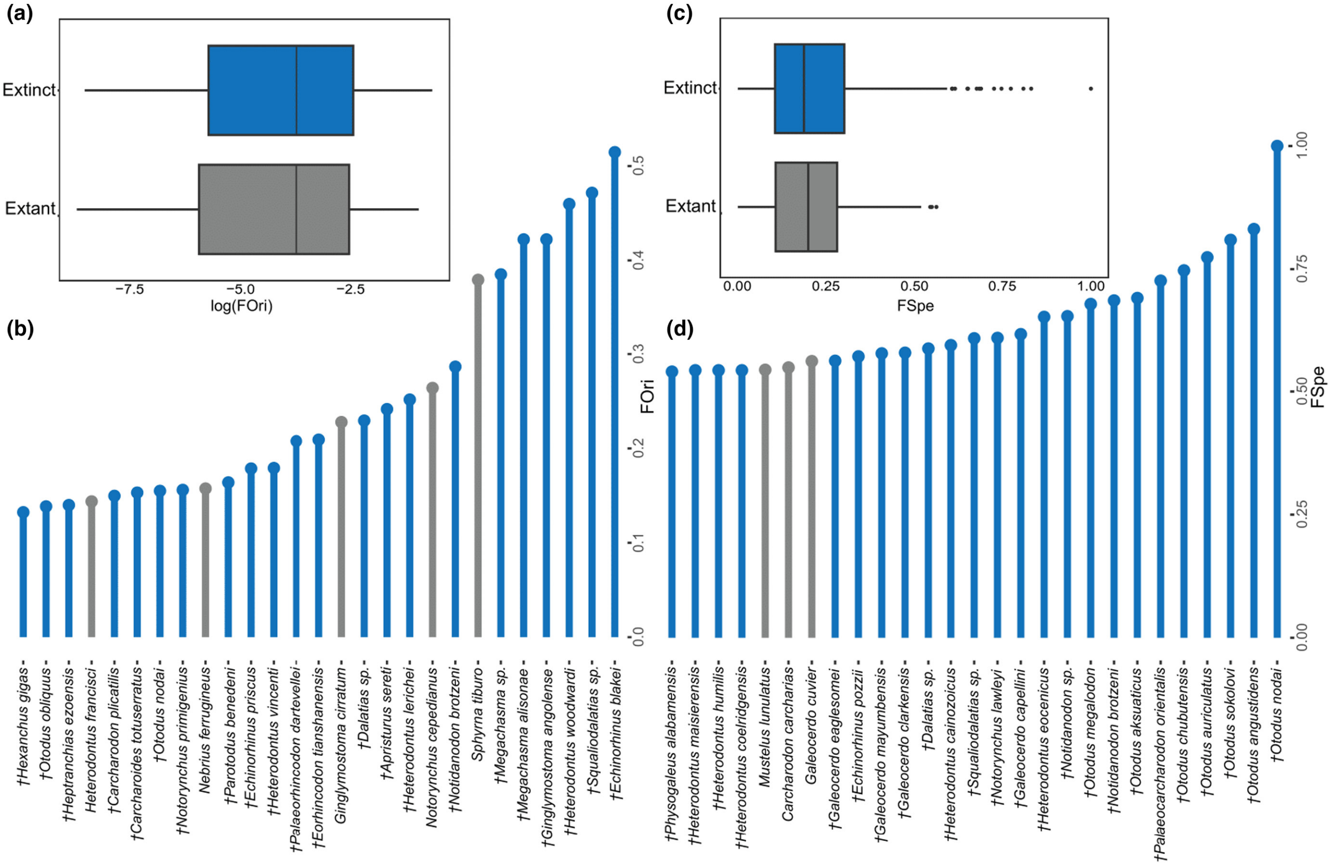

FIGURE 3 Functional originality (FOri) and specialization (FSpe) of extinct and extant Cenozoic sharks. (a) mean FOri, log transformed for visualization; (b) top 5% FOri taxa; (c) mean FSpe; (d) top 5% FSpe taxa. Taxa are coloured based on their status as extinct (blue) or extant (grey).

3.3.2 | Functionally original taxa

In the Palaeocene, the highest scoring FOri taxon was an extinct kitefin shark †*Squaliodatalias* sp., which occupied the lower end of PCoA1 and PCoA2 (Figure 1b), denoting small, smooth and piercing teeth with lateral cusplets. Based on Cooper et al. (2023), this indicates a prey preference for invertebrates and a clutching feeding mechanism. The Eocene's highest scoring FOri species was an extinct bullhead shark †*Heterodontus woodwardi*, which occupied intermediate trait values along PCoA1, and the lowest values along PCoA2 (Figure 1c). This represents small, semi-circular teeth with no lateral cusplets or cutting edge, typical of a crushing feeding mechanism and a hard-shelled invertebrate prey preference seen also in its living representatives (Cooper et al., 2023; Hovestadt, 2018). The extinctions of †*Squaliodalatias* sp. and †*H. woodwardi* did not result in gaps in the functional space as close neighbours playing similar ecological roles survived (Figure 1b–d). The most functionally original taxon of the Oligocene was †*Dalatias* sp., a kitefin shark which occupied intermediate trait values along PCoA2 (Figure 1e), marking medium-sized teeth with serrated cutting edges and thus suggesting a medium body size and prey preference for fishes (Cooper et al., 2023). Today, there is a single extant species of this genus, *Dalatias licha*, which occupies a high trophic level due to being able to occasionally take bites out of prey larger than itself (Navarro et al., 2014). Although *D. licha* has a fossil record dating as far back as the Eocene (Paillard et al., 2020), †*Dalatias* sp. differed in space by occupying higher trait values along PCoA2, implying larger, more heavily serrated teeth (Cooper et al., 2023). We therefore consider this taxon extinct and separately from its living counterpart. This taxon persisted into the Pleistocene, but its absence from the Recent sample left a significant gap in the functional space (Figure 1g,h), indicating the loss of a distinct ecological role played by mid-sized deep-sea predators.

The highest scoring FOri species in the Miocene and Pliocene was an extinct bramble shark †*Echinorhinus blakei*, which was also the most functionally original of the whole Cenozoic (Figure 3b). This species occupied low trait values along PCoA1 (Figure 1e,f), denoting piercing longitudinal outlines and lateral cusplets, and indicating a clutching and grasping feeding mechanism (Cooper et al., 2023). However, this species also occupied intermediate values along PCoA2, marking smooth cutting edges and medium crown heights, implying a medium body size and a prey preference of fishes (Cooper et al., 2023). Indeed, Echinorhiniformes was the order with the highest mean FOri (Figure S12a). Both extinct and extant echinorhiniforms are poorly studied (Bogan & Agnolín, 2022), but the order is known for medium to large body sizes (reaching 4–4.5 m long) and suction feeding (Ebert et al., 2021). Notably, the extinction of †*E. blakei* between the Pliocene and Pleistocene left a gap in the shark functional space (Figure 1g,h), indicating the loss of an ecological role played by medium-sized suction feeders. A megamouth shark, †*Megachasma* sp., was the most functionally original taxon of the Pleistocene, and occupied low PCoA1 values (Figure 1g), denoting teeth with lateral cusplets and piercing longitudinal outlines and thus a clutching or vestigial morphology, typical of a filter feeding mechanism (Cooper et al., 2023). The space left by †*Megachasma* sp. was retained in the Recent by close neighbours with similar ecological roles. The highest scoring FOri species of the Recent sample was the bonnethead shark *Sphyrna tiburo*. This species occupied intermediate trait values along PCoA1 and the lowest values along PCoA2 (Figure 1h), indicating small, semi-circular teeth with no cutting edge or lateral cusplets, and thus suggesting crushing feeding and prey preferences of invertebrates (Cooper et al., 2023), in line with the species' known ecology (Leigh et al., 2018; Mara et al., 2010).

Overall, our results suggest that mid-sized sharks feeding on invertebrates and fishes displayed high FOri values, and thus were highly isolated in trait space through time. The Pliocene extinction of †*E. blakei*, a presumed mid-sized suction feeder, and the Pleistocene extinction of †*Dalatias* sp., a presumed mid-sized piscivore, left the largest gaps in the trait space.

3.3.3 | Functionally specialized taxa

The highest scoring FSpe taxa of the Palaeocene and Eocene epochs were †*Palaeocarcharodon orientalis* and †*Otodus nodai*, respectively, with †*O. nodai* also being the most functionally specialized species of the Cenozoic (Figures 1b,c and 3d). These species sat in the upper end of PCoA2 (Figure 1c,d), denoting a prey preference for high vertebrates based on their large and serrated teeth (Cooper et al., 2023). The extinction of these species did not result in the loss of functional space, as other taxa playing similar macropredatory ecological roles occupied neighbouring sections of the space (Figure 1b–d). The highest scoring FSpe species of the Oligocene and Miocene was †*O. angustidens*, which was a close neighbour of †*O. nodai* from the Eocene (Figure 1d,e) and had an inferred prey preference of high vertebrates (Cooper et al., 2023). The extinction of this species in the Miocene resulted in the loss of the highest trait values along PCoA2 (Figure 1e,f). †*O. megalodon* was the highest FSpe species of the Pliocene, occupying the highest end of PCoA1 (Figure 1f). This marks triangular teeth with no lateral cusplets and thus a cutting feeding mechanism (Cooper et al., 2023). †*O. megalodon*'s extinction in the Pliocene left a notable gap in the Pleistocene trait space (Figure 1f,g). Overall, the extinctions of the different †*Otodus* species in the Miocene and Pliocene resulted in the loss of ecological roles played by giant apex predators. The highest FSpe taxon of the Pleistocene was †*Dalatias* sp. (Figure 1g), which occupied the highest remaining values along PCoA2. The absence of this taxon in the Recent suggests a further loss of predatory ecological roles (Figure 1g,h). This left the tiger shark *Galeocerdo cuvier* as the most functionally specialized species of the Recent, which occupied high values along PCoA1 (Figure 1h), marking teeth with polygonal longitudinal outlines and no lateral cusplets; and a cutting feeding mechanism (Cooper et al., 2023).

The most functionally specialized taxa of the Cenozoic belong to the orders Squaliformes (†*Dalatias* sp.), Carcharhiniformes (*G. cuvier*) and Lamniformes (†*P. orientalis* and †*Otodus* spp.). While none of these orders had the highest mean FSpe scores, all had high-ranking outliers represented by the above-mentioned taxa and others, particularly Lamniformes (Figure S12b). These results collectively indicate that the Miocene–Pliocene extinctions of †*Otodus* species, followed by the Pleistocene extinction of †*Dalatias* sp. (i.e. the reduction of the *Dalatias* genus to a single living species; *D. licha*), were probable drivers of functional diversity losses between the Miocene and the Recent.

Overall, when examining the contributions of individual taxa to the Cenozoic functional diversity, our results revealed that (1) extinct sharks spanned a larger extent of the functional space and were generally more functionally distinct than extant sharks (Figures 1i and 3); and (2) specialized suction feeders, mid-sized deep-sea predators and gigantic apex predators were important contributors to functional diversity, with their Miocene-Pleistocene extinctions resulting in losses inside the functional space, likely explaining the overall decline of functional diversity from the late Miocene onwards (Figures 1f–h, 2, and S6).

4 | CONCLUSIONS

Our tooth-based analyses revealed that shark functional diversity was generally high throughout most of the Cenozoic (e.g. FRic >60%; Table 1), peaking at 86%–87% FRic in the Eocene and Miocene (56–33.9 and 23.03–5.333 Ma; Figures 1c,e, 2d, and S6). Despite the loss of species in the K/Pg (Guinot & Condamine, 2023; Kriwet & Benton, 2004), shark functional diversity was higher than expected between the Palaeocene and Miocene epochs (FRic $Z > 1.96$ in the Palaeocene, Oligocene and Miocene; Table 2). However, we found that shark functional diversity has steadily declined since its Miocene peak, with 44% of FRic being lost between then and the present (Tables 1 and S7; Figures 1e–h, 2d, and S6d). Consequently, shark functional diversity today is likely diminished compared with the Cenozoic past. Indeed, we found that extinct sharks inordinately contributed to functional diversity compared with extant sharks (Figures 1i and 3). The functional diversity decline from the late Miocene onwards was likely driven by the loss of giant apex predators (i.e. †*Otodus* spp. in the Miocene and Pliocene), suction feeders (e.g. †*Echinorhinus blakei* in the Pliocene) and deep-sea sharks at high trophic levels (i.e. the extinction of †*Dalatias* sp. in the Pleistocene). Today, sharks rank among the most imperilled marine vertebrates on Earth, with overfishing emerging as the primary driver of extinction (Dulvy et al., 2014, 2021; Stein et al., 2018). Our findings forewarn that ongoing anthropogenic-driven shark declines might be eroding an already diminished functional diversity. Current recommendations to safeguard elasmobranch functional diversity include the identification of functionally unique, specialized and endangered species, as well as the areas harbouring hotspots of functional diversity (Pimiento et al., 2023). Our study further highlights the modern shark species holding some of the Cenozoic functional space, potentially complementing our knowledge on the current priorities for the preservation of shark functional diversity in the changing world.

AUTHOR CONTRIBUTIONS

CP conceived the project. Both authors designed the research. JAC collected the data, performed all analyses and wrote the first versions of the manuscript with guidance and input from CP.

ACKNOWLEDGEMENTS

We thank the following museum curators and staff for access to specimens: E. Bernard and J. Maclaine (NHM); U. Gohlich and A. Palandacic (NHMW); C. Klug (PIMUZ); R. Kindlimann (RKC); A. Folie and O. Pauwels (RBINS); S. Godfrey, J. Nance and V. Perez (CMM); B. MacFadden (UF); G. Hubbell (GHC) and R. Salas-Gismondi and A. Altamirano-Sierra (MUSM). We additionally thank J. N. Griffin, G. Mathes, K. Kocáková, C. Magneville and T. Lewis for their advice and assistance. Finally, we thank the editor K. Lyons and two anonymous reviewers for their constructive comments that significantly improved this manuscript. JAC was funded by a PhD studentship from the Fisheries Society of the British Isles and an international travel grant from the University of Florida. CP is funded by a PRIMA grant (no. 185798) from the Swiss National Science Foundation.

CONFLICT OF INTEREST STATEMENT

The authors declare that they have no competing interests.

DATA AVAILABILITY STATEMENT

The data used in this study are included as supplementary material (Data S1 and S2). All images of all specimens used in this study are available via Zenodo at https://doi.org/10.5281/zenodo.10076354. All R code used to conduct the analyses are available via GitHub at https://github.com/Pimiento-Research-Group/Shark-FD-through-time.

ORCID

Jack A. Cooper https://orcid.org/0000-0003-2252-4983
Catalina Pimiento http://orcid.org/0000-0002-5320-7246

REFERENCES

Abràmoff, M. D., Magalhães, P. J., & Ram, S. J. (2004). Image processing with ImageJ. *Biophotonics International*, *11*, 36–42.

Albert, C. H., de Bello, F., Boulangeat, I., Pellet, G., Lavorel, S., & Thuiller, W. (2012). On the importance of intraspecific variability for the quantification of functional diversity. *Oikos*, *121*, 116–126.

Alfaro, M. E., Faircloth, B. C., Harrington, R. C., Sorenson, L., Friedman, M., Thacker, C. E., Oliveros, C. H., Cerny, D., & Near, T. J. (2018). Explosive diversification of marine fishes at the Cretaceous-Palaeogene boundary. *Nature Ecology and Evolution*, *2*, 688–696.

Alroy, J., Aberhan, M., Bottjer, D. J., Foote, M., Fürsich, F. T., Harries, P. J., Hendy, A. J., Holland, S. M., Ivany, L. C., Kiessling, W., Kosnik, M. A., Marshall, C. R., McGowan, A. J., Miller, A. I., Olszewski, T. D., Patzkowsky, M. E., Peters, S. E., Villier, L., Wagner, P. J., … Visaggi, C. C. (2008). Phanerozoic trends in the global diversity of marine invertebrates. *Science*, *321*, 97–100.

Bazzi, M., Campione, N. E., Kear, B. P., Pimiento, C., & Ahlberg, P. E. (2021). Feeding ecology has shaped the evolution of modern sharks. *Current Biology*, *31*, 1–11.

Belben, R. A., Underwood, C. J., Johanson, Z., & Twitchett, R. J. (2017). Ecological impact of the end-cretaceous extinction on lamniform sharks. *PLoS One*, *12*, e0178294.

Benton, M. J., Dunhill, A. M., Lloyd, G. T., & Marx, F. G. (2011). Assessing the quality of the fossil record: Insights from vertebrates. *Geological Society, London, Special Publications*, *358*, 63–94.

Boessenecker, R. W., Ehret, D. J., Long, D. J., Churchill, M., Martin, E., & Boessenecker, S. J. (2019). The early Pliocene extinction of the mega-toothed shark *Otodus megalodon*: A view from the eastern North Pacific. *PeerJ*, *7*, e6088.

Bogan, S., & Agnolín, F. L. (2022). The fossil record of the Bramble-shark *Echinorhinus* (Echinorhiniformes, Echinorhinidae) in South America. *Journal of South American Earth Sciences*, *120*, 104083.

Burke, K. D., Williams, J. W., Chandler, M. A., Haywood, A. M., Lunt, D. J., & Otto-Bliesner, B. L. (2018). Pliocene and Eocene provide best analogs for near-future climates. *Proceedings of the National Academy of Sciences*, *115*, 13288–13293.

Cappetta, H. (2012). Handbook of Paleoichthyology—Chondrichthyes—Mesozoic and Cenozoic Elasmobranchii: Teeth. In H.-P. Schultze (Ed.), *Handbook of paleoichthyology* (Vol. *3E*, pp. 1–512). Verlag Dr. Friedrich Pfiel.

Ciampaglio, C. N., Wray, G. A., & Corliss, B. H. (2005). A toothy tale of evolution: convergence in tooth morphology among marine Mesozoic–Cenozoic sharks, reptiles, and mammals. *The Sedimentary Record*, *3*, 4–8.

Cianciaruso, M. V., Batalha, M. A., Gaston, K. J., & Petchey, O. L. (2009). Including intraspecific variability in functional diversity. *Ecology*, *90*, 81–89.

Collareta, A., Lambert, O., Landini, W., Di Celma, C., Malinverno, E., Varas-Malca, R., Urbina, M., & Bianucci, G. (2017). Did the giant extinct shark *Carcharocles megalodon* target small prey? Bite marks on marine mammal remains from the late Miocene of Peru. *Palaeogeography, Palaeoclimatology, Palaeoecology*, *469*, 84–91.

Compagno, L. J. V. (1990). Alternative life-history styles of cartilaginous fishes in time and space. *Environmental Biology of Fishes*, *28*, 33–75.

Cooke, R., Gearty, W., Chapman, A. S. A., Dunic, J., Edgar, G. J., Lefcheck, J. S., Rilov, G., McClain, C. R., Stuart-Smith, R. D., Lyons, S. K., & Bates, A. E. (2022). Anthropogenic disruptions to longstanding patterns of trophic-size structure in vertebrates. *Nature Ecology and Evolution*, *6*, 684–692.

Cooper, J. A., Griffin, J. N., Kindlimann, R., & Pimiento, C. (2023). Are shark teeth proxies for functional traits? A framework to infer ecology from the fossil record. *Journal of Fish Biology*, *103*, 798–814.

Cooper, J. A., Hutchinson, J. R., Bernvi, D. C., Cliff, G., Wilson, R. P., Dicken, M. L., Menzel, J., Wroe, S., Pirlo, J., & Pimiento, C. (2022). The extinct shark *Otodus megalodon* was a transoceanic superpredator: Inferences from 3D modeling. *Science*. *Advances*, *8*, eabm9424.

Cortés, E. (1999). Standardized diet compositions and trophic levels of sharks. *ICES Journal of Marine Science*, *56*, 707–717.

Coulon, N., Elliott, S., Teichert, N., Auber, A., McLean, M., Barreau, T., Feunteun, E., & Carpentier, A. (2024). Northeast Atlantic elasmobranch community on the move: Functional reorganization in response to climate change. *Global Change Biology*, *30*, e17157.

Cullen, J. A., & Marshall, C. D. (2019). Do sharks exhibit heterodonty by tooth position and over ontogeny? A comparison using elliptic Fourier analysis. *Journal of Morphology*, *280*, 687–700.

de Bello, F., Botta-Dukát, Z., Lepš, J., Fibich, P., & Goslee, S. (2020). Towards a more balanced combination of multiple traits when computing functional differences between species. *Methods in Ecology and Evolution*, *12*, 443–448.

de Bello, F., Lavorel, S., Albert, C. H., Thuiller, W., Grigulis, K., Dolezal, J., Janeček, Š., & Lepš, J. (2011). Quantifying the relevance of intraspecific trait variability for functional diversity. *Methods in Ecology and Evolution*, *2*, 163–174.

De Boer, B., Van de Wal, R., Bintanja, R., Lourens, L., & Tuenter, E. (2010). Cenozoic global ice-volume and temperature simulations with 1-D ice-sheet models forced by benthic δ 18 O records. *Annals of Glaciology*, *51*, 23–33.

Dulvy, N. K., Fowler, S. L., Musick, J. A., Cavanagh, R. D., Kyne, P. M., Harrison, L. R., Carlson, J. K., Davidson, L. N., Fordham, S. V., Francis, M. P., Pollock, C. M., Simpfendorfer, C. A., Burgess, G. H., Carpenter, K. E., Compagno, L. J. V., Ebert, D. A., Gibson, C., Heupel, M. R., Livingstone, S. R., … White, W. T. (2014). Extinction risk and conservation of the world's sharks and rays. *eLife*, *3*, e00590.

Dulvy, N. K., Pacoureau, N., Rigby, C. L., Pollom, R. A., Jabado, R. W., Ebert, D. A., Finucci, B., Pollock, C. M., Cheok, J., Derrick, D. H., Herman, K. B., Sherman, C. S., VanderWright, W. J., Lawson, J. M., Walls, R. H. L., Carlson, J. K., Charvet, P., Bineesh, K. K., Fernando, D., … Simpfendorfer, C. A. (2021). Overfishing drives over one-third of all sharks and rays toward a global extinction crisis. *Current Biology*, *31*, 4773–4787.

Ebert, D. A., Dando, M., & Fowler, S. (2021). *Sharks of the world: A complete guide*. Princeton University Press.

Foote, M., & Sepkoski, J. J. (1999). Absolute measures of the completeness of the fossil record. *Nature*, *398*, 415–417.

Friedman, M., & Sallan, L. C. (2012). Five hundred million years of extinction and recovery: A phanerozoic survey of large-scale diversity patterns in fishes. *Palaeontology*, *55*, 707–742.

Garcia, V. B., Lucifora, L. O., & Myers, R. A. (2008). The importance of habitat and life history to extinction risk in sharks, skates, rays and chimaeras. *Proceedings of the Royal Society B*, *275*, 83–89.

Godfrey, S. J., & Beatty, B. L. (2022). A Miocene cetacean vertebra showing a partially healed longitudinal shear-compression fracture, possibly the result of domoic acid toxicity or failed predation. *Palaeontologia Electronica*, *25*, a28.

Godfrey, S. J., Nance, J. R., & Riker, N. L. (2021). *Otodus*-bitten sperm whale tooth from the Neogene of the Coastal Eastern United States. *Acta Palaeontologica Polonica*, *66*, 599–603.

Gower, J. C. (1971). A general coefficient of similarity and some of its properties. *Biometrics*, *27*, 857.

Gradstein, F. M., Ogg, J. G., Schmitz, M. D., & Ogg, G. M. (2012). *The geologic time scale 2012*. Elsevier.

Griffin, J. N., Leprieur, F., Silvestro, D., Lefcheck, J. S., Albouy, C., Rasher, D. B., Davis, M., Svenning, J.-C., & Pimiento, C. (2020). Functionally unique, specialised, and endangered (FUSE) species: Towards integrated metrics for the conservation prioritisation toolbox. *BioRxiv* 2020.05.09.084871.

Guinot, G., Adnet, S., & Cappetta, H. (2012). An analytical approach for estimating fossil record and diversification events in sharks, skates and rays. *PLoS ONE*, *7*, e44632.

Guinot, G., & Cavin, L. (2016). 'Fish' (Actinopterygii and Elasmobranchii) diversification patterns through deep time. *Biological Reviews*, *91*, 950–981.

Guinot, G., & Condamine, F. L. (2023). Global impact and selectivity of the Cretaceous-Paleogene mass extinction among sharks, skates and rays. *Science*, *379*, 802–806.

Hedberg, C. P., Lyons, S. K., & Smith, F. A. (2021). The hidden legacy of megafaunal extinction: Loss of functional diversity and resilience over the Late Quaternary at Hall's Cave. *Global Ecology and Biogeography*, *31*, 294–307.

Hovestadt, D. C. (2018). Reassessment and revision of the fossil Heterodontidae (Chondrichthyes: Neoselachii) based on tooth morphology of extant taxa. *Palaeontos*, *30*, 3–120.

IUCN. (2023). The IUCN red list of threatened species. www.iucnredlist.org

Kast, E. R., Griffiths, M. L., Kim, S. L., Rao, Z. C., Shimada, K., Becker, M. A., Maisch, H. M., Eagle, R. A., Clarke, C. A., Neumann, A. N., Karnes, M. E., Lüdecke, T., Leichliter, J. N., Martínez-García, A., Akhtar, A. A., Wang, X. T., Haug, G. H., & Sigman, D. M. (2022).

Cenozoic megatooth sharks occupied extremely high trophic positions. *Science Advances*, *8*, eabl6529.

Kent, B. W. (1994). *Fossil sharks of the Chesapeake Bay region*. Egan Rees & Boyer, Inc.

Kent, B. W. (2018). The cartilaginous fishes (chimaeras, sharks and rays) of Calvert Cliffs, Maryland, USA. In S. J. Godfrey (Ed.), *The geology and vertebrate paleontology of Calvert Cliffs, Maryland, USA* (pp. 45–157). Smithsonian Institution Scholarly Press.

Kriwet, J., & Benton, M. J. (2004). Neoselachian (Chondrichthyes, Elasmobranchii) diversity across the Cretaceous–Tertiary boundary. *Palaeogeography, Palaeoclimatology, Palaeoecology*, *214*, 181–194.

Lefcheck, J. S., Bastazini, V. A. G., & Griffin, J. N. (2015). Choosing and using multiple traits in functional diversity research. *Environmental Conservation*, *42*, 104–107.

Leigh, S. C., Papastamatiou, Y. P., & German, D. P. (2018). Seagrass digestion by a notorious 'carnivore'. *Proceedings of the Royal Society B*, *285*, 20181583.

Magneville, C., Loiseau, N., Albouy, C., Casajus, N., Claverie, T., Escalas, A., Leprieur, F., Maire, E., Mouillot, D., & Villéger, S. (2022). mFD: An R package to compute and illustrate the multiple facets of functional diversity. *Ecography*, *2022*, e05904.

Maire, E., Grenouillet, G., Brosse, S., & Villéger, S. (2015). How many dimensions are needed to accurately assess functional diversity? A pragmatic approach for assessing the quality of functional spaces. *Global Ecology and Biogeography*, *24*, 728–740.

Mara, K. R., Motta, P. J., & Huber, D. R. (2010). Bite force and performance in the durophagous bonnethead shark, *Sphyrna tiburo*. *Journal of Experimental Zoology Part A: Ecological Genetics and Physiology*, *313*, 95–105.

Marshall, C. R. (2019). Using the fossil record to evaluate timetree timescales. *Frontiers in Genetics*, *10*, 1049.

Marx, F. G., & Uhen, M. D. (2010). Climate, critters, and cetaceans: Cenozoic drivers of the evolution of modern whales. *Science*, *327*, 993–996.

Miller, K. G., Kominz, M. A., Browning, J. V., Wright, J. D., Mountain, G. S., Katz, M. E., Sugarman, P. J., Cramer, B. S., Christie-Blick, N., & Pekar, S. F. (2005). The Phanerozoic record of global sea-level change. *Science*, *310*, 1293–1298.

Mouillot, D., Graham, N. A., Villéger, S., Mason, N. W., & Bellwood, D. R. (2013). A functional approach reveals community responses to disturbances. *Trends in Ecology and Evolution*, *28*, 167–177.

Mouillot, D., Villéger, S., Parravicini, V., Kulbicki, M., Arias-Gonzalez, J. E., Bender, M., Chabanet, P., Floeter, S. R., Friedlander, A., Vigliola, L., & Bellwood, D. R. (2014). Functional over-redundancy and high functional vulnerability in global fish faunas on tropical reefs. *Proceedings of the National Academy of Sciences*, *111*, 13757–13762.

Munroe, S. E. M., Simpfendorfer, C. A., & Heupel, M. R. (2013). Defining shark ecological specialisation: Concepts, context, and examples. *Reviews in Fish Biology and Fisheries*, *24*, 317–331.

Myers, R. A., Baum, J. K., Shepherd, T. D., Powers, S. P., & Peterson, C. H. (2007). Cascading effects of the loss of apex predatory sharks from a coastal ocean. *Science*, *315*, 1846–1850.

Navarro, J., López, L., Coll, M., Barría, C., & Sáez-Liante, R. (2014). Short- and long-term importance of small sharks in the diet of the rare deep-sea shark *Dalatias licha*. *Marine Biology*, *161*, 1697–1707.

Navia, A. F., Mejía-Falla, P. A., López-García, J., Giraldo, A., & Cruz-Escalona, V. H. (2017). How many trophic roles can elasmobranchs play in a marine tropical network? *Marine and Freshwater Research*, *68*, 1342–1353.

Paillard, A., Shimada, K., & Pimiento, C. (2020). The fossil record of extant elasmobranchs. *Journal of Fish Biology*, *98*, 445–455.

Pavoine, S., Vallet, J., Dufour, A.-B., Gachet, S., & Daniel, H. (2009). On the challenge of treating various types of variables: Application for improving the measurement of functional diversity. *Oikos*, *118*, 391–402.

Pimiento, C., Albouy, C., Silvestro, D., Mouton, T. L., Velez, L., Mouillot, D., Judah, A. B., Griffin, J. N., & Leprieur, F. (2023). Functional diversity of sharks and rays is highly vulnerable and supported by unique species and locations worldwide. *Nature Communications*, *14*, 7691.

Pimiento, C., & Benton, M. J. (2020). The impact of the pull of the recent on extant elasmobranchs. *Palaeontology*, *63*, 369–374.

Pimiento, C., & Clements, C. F. (2014). When did *Carcharocles megalodon* become extinct? A new analysis of the fossil record. *PLoS ONE*, *9*, e111086.

Pimiento, C., Griffin, J. N., Clements, C. F., Silvestro, D., Varela, S., Uhen, M. D., & Jaramillo, C. (2017). The Pliocene marine megafauna extinction and its impact on functional diversity. *Nature Ecology and Evolution*, *1*, 1100–1106.

Pimiento, C., Leprieur, F., Silvestro, D., Lefcheck, J. S., Albouy, C., Rasher, D. B., Davis, M., Svenning, J.-C., & Griffin, J. N. (2020). Functional diversity of marine megafauna in the Anthropocene. *Science Advances*, *6*, eaay7650.

Pimiento, C., MacFadden, B. J., Clements, C. F., Varela, S., Jaramillo, C., Velez-Juarbe, J., & Silliman, B. R. (2016). Geographical distribution patterns of *Carcharocles megalodon* over time reveal clues about extinction mechanisms. *Journal of Biogeography*, *43*, 1645–1655.

Pollerspöck, J., & Straube, N. (2014). Shark-references. www.shark-references.com

R Development Core Team. (2017). *R: A language and environment for statistical computing*. R Foundation for Statistical Computing.

Rabosky, D. L., & Sorhannus, U. (2009). Diversity dynamics of marine planktonic diatoms across the Cenozoic. *Nature*, *457*, 183–186.

Raja, N. B., Dunne, E. M., Matiwane, A., Khan, T. M., Natscher, P. S., Ghilardi, A. M., & Chattopadhyay, D. (2022). Colonial history and global economics distort our understanding of deep-time biodiversity. *Nature Ecology & Evolution*, *6*, 145–154.

Rummer, J. L., Bouyoucos, I. A., Wheeler, C. R., Santos, C. P., & Rosa, R. (2022). Climate change and sharks. In J. C. Carrier, C. A. Simpfendorfer, M. R. Heithaus, & K. E. Yopak (Eds.), *Biology of sharks and their relatives* (pp. 767–793). CRC Press.

Shimada, K., & Ward, D. J. (2016). The oldest fossil record of the megamouth shark from the late Eocene of Denmark, and comments on the enigmatic megachasmid origin. *Acta Palaeontologica Polonica*, *61*, 839–845.

Sibert, E. C., & Norris, R. D. (2015). New age of fishes initiated by the Cretaceous-Paleogene mass extinction. *Proceedings of the National Academy of Sciences*, *112*, 8537–8542.

Sibert, E. C., & Rubin, L. D. (2021). An early Miocene extinction in pelagic sharks. *Science*, *372*, 1105–1107.

Signorell, A., Aho, K., Alfons, A., Anderegg, N., Aragon, T., Arppe, A., Baddeley, A., Barton, K., Bolker, B., & Borchers, H. W. (2019). DescTools: Tools for descriptive statistics. *R package version 0.99*, *28*, 17.

Smith, S. J., Edmonds, J., Hartin, C. A., Mundra, A., & Calvin, K. (2015). Near-term acceleration in the rate of temperature change. *Nature Climate Change*, *5*, 333–336.

Stein, R. W., Mull, C. G., Kuhn, T. S., Aschliman, N. C., Davidson, L. N. K., Joy, J. B., Smith, G. J., Dulvy, N. K., & Mooers, A. O. (2018). Global priorities for conserving the evolutionary history of sharks, rays and chimaeras. *Nature Ecology & Evolution*, *2*, 288–298.

Uhen, M. D. (2007). Evolution of marine mammals: Back to the sea after 300 million years. *The Anatomical Record*, *290*, 514–522.

Villéger, S., Mason, N. W., & Mouillot, D. (2008). New multidimensional functional diversity indices for a multifaceted framework in functional ecology. *Ecology*, *89*, 2290–2301.

Villéger, S., Novack-Gottshall, P. M., & Mouillot, D. (2011). The multidimensionality of the niche reveals functional diversity changes in benthic marine biotas across geological time. *Ecology Letters*, *14*, 561–568.

Weigmann, S. (2016). Annotated checklist of the living sharks, batoids and chimaeras (Chondrichthyes) of the world, with a focus on biogeographical diversity. *Journal of Fish Biology*, *88*, 837–1037.

Williams, J. J., Papastamatiou, Y. P., Caselle, J. E., Bradley, D., & Jacoby, D. M. P. (2018). Mobile marine predators: An understudied source of nutrients to coral reefs in an unfished atoll. *Proceedings of the Royal Society B*, *285*, 20172456.

Zachos, J., Pagani, M., Sloan, L., Thomas, E., & Billups, K. (2001). Trends, rhythms, and aberrations in global climate 65 Ma to present. *Science*, *292*, 686–693.

SUPPORTING INFORMATION

Additional supporting information can be found online in the Supporting Information section at the end of this article.

How to cite this article: Cooper, J. A., & Pimiento, C. (2024). The rise and fall of shark functional diversity over the last 66 million years. *Global Ecology and Biogeography*, *00*, e13881. https://doi.org/10.1111/geb.13881